European Congress on Computational Methods in Applied Sciences and Engineering
ECCOMAS 2004
P. Neittaanmäki, T. Rossi, K. Majava, and O. Pironneau (eds.)
W. Rodi and P. Le Quéré (assoc. eds.)
Jyväskylä, 24—28 July 2004

THE EFFICIENCY OF GAS-KINETIC BGK SCHEME FOR SOLVING 2-D COMPRESSIBLE INVISCID REGULAR SHOCK REFLECTION PROBLEM

Ong J. Chit[§], Ashraf A. Omar[¤], Waqar Asrar[¢] and Megat M. Hamdan[£]

[§]Department of Aerospace Engineering
[£]Department of Mechanical & Manufacturing Engineering
Faculty of Engineering, University Putra Malaysia, 43400 Serdang, Selangor D.E., Malaysia

[¤¢]Department of Mechanical Engineering
Faculty of Engineering, International Islamic University Malaysia, Jalan Gombak, 53100 Kuala Lumpur, Malaysia
e-mails: [¤]aao@iiu.edu.my

Key words: Compressible Inviscid Flow, Gas-Kinetic Schemes, BGK scheme, High Resolution Scheme.

Abstract. *In this paper, the 1st and 2nd order gas-kinetic BGK scheme is developed and tested for its ability in solving the two-dimensional compressible inviscid flow fields. The BGK (Bhatnagar-Gross-Krook) scheme uses the collisional Boltzmann equation as the governing equation for flow evolutions. Second-order BGK scheme is also developed for flow simulation. This is achieved by means of reconstructing the initial data via MUSCL (Monotone Upstream-Centered Schemes for Conservation Laws) method. In addition, a multisage TVD (Total Variation Diminishing) Runge-Kutta method is employed for the time integration of the finite volume gas-kinetic scheme. A typical two-dimensional regular reflection of an oblique shock wave from a solid surface is chosen for testing the accuracy and robustness of the BGK scheme. The computational results are validated against the numerical results of Roe's scheme.*

1 INTRODUCTION

The development of numerical schemes for compressible simulations has attracted much attention in the past years. Godunov-type schemes and flux vector splitting schemes are among those most notable and successful numerical schemes. In the family of Godunov-type schemes, Roe's FDS (Flux Difference Splitting) scheme [8] has enjoyed great popularity owing to its accuracy for simulating compressible inviscid flows. Through this method, the average state flux Jacobian satisfying the Rankine-Hugoniot relation is introduced to solve exactly the locally linearized Euler equations and can capture a shock within one computational cell.

A typical Godunov-type finite volume scheme has two stages [1], reconstruction stage for constructing initial cell-averaged values at cell interfaces and evolution stage for computing flow variables at later times by solving the physical governing equations. The evolution stage of the Godunov-type scheme is based on the Riemann solution, while the gas-kinetic scheme is based on the simplified Boltzmann equation [3]. The BGK scheme is different from other Bolzmann-type schemes, which solve the collisionless Boltzmann equation by neglecting the collision term of the Boltzmann equation. With the inclusion of collision term in the Boltzmann equation, the BGK scheme take into account the particle collisions in the whole gas evolution process within a time step, from which a time-dependent gas distribution function and the resulting numerical fluxes at the cell interface are obtained [9]. A particular strength of the BGK scheme lies precisely where most Godunov-type FDS schemes often fail, such as carbuncle phenomenon, positivity, and entropy condition.

The advancement of gas-kinetic BGK scheme for compressible flow simulations and other applications has attracted much attention and become matured in the last decade. Xu [3] introduced Jameson's SLIP formulation to construct high-order BGK schemes. In 2000, Chae [10] and Kim proposed a modified gas-kinetic BGK scheme by introducing the Prantl number correction into flux calculations. While in 2002, Yeefeng [9] and Jameson extended the gas-kinetic BGK scheme to three-dimensional compressible flows. Lately Xu [4] has used BGK scheme to solve ideal MHD equations.

In this paper, the authors will present numerical results for the two-dimensional compressible inviscid regular shock reflection problem in term of first- and second-order accuracy of the BGK scheme. Then, these results are validated via Roe's scheme.

2 GAS-KINETIC THEORY

The hydrodynamic equations for two-dimensional system of Euler equations are given by

$$\partial_t W + \partial_x F(W) + \partial_y G(W) = 0, \tag{1}$$

where

$$W = \begin{bmatrix} \rho \\ \rho U \\ \rho V \\ \rho \varepsilon \end{bmatrix}, \quad F(W) = \begin{bmatrix} \rho U \\ \rho U^2 + p \\ \rho UV \\ \rho \varepsilon U + pU \end{bmatrix}, \quad G(W) = \begin{bmatrix} \rho V \\ \rho UV \\ \rho V^2 + p \\ \rho \varepsilon V + pV \end{bmatrix}$$

Where ρ, ρU, ρV and $\rho \varepsilon$ are the mass, x-momentum, y-momentum and energy density respectively and p is the pressure. The Euler equations could be approximated by the Bolztmann equation in the gas evolution stage [2,3].

The Boltzmann equation in the two-dimensional case is

$$f_t + uf_x + vf_y = Q(f, f), \tag{2}$$

where f is the gas-distribution function, u and v the particle velocities, and $Q(f, f)$ is the collision term. The collision term is an integral function, which accounts for the binary collisions. In most cases, the collision term can be simplified and the BGK model is one of them,

$$Q(f, f) = (g - f)/\tau, \tag{3}$$

where g are the equilibrium state and τ the collision time.

The Euler equations could only be recovered from the Boltzmann equation when the equilibrium state g, is a Maxwellian:

$$g = \rho\left(\frac{\lambda}{\pi}\right)^{\frac{K+2}{2}} e^{-\lambda\left((u-U)^2 + \left(v-V^2\right) + \xi^2\right)}, \tag{4}$$

where ξ is a K dimensional vector, which accounts for the internal degrees of freedom, such as molecular rotation and vibrations, and $\xi^2 = \xi_1^2 + \xi_2^2 + \ldots + \xi_K^2$, U and V are the corresponding macroscopic flow velocities in the x- and y-direction respectively. The dimensional vector, K is related to the specific heat ratio γ, and for two-dimensional gas flow,

$$K = (4 - 2\gamma)/(\gamma - 1), \tag{5}$$

where, for a diatomic gas $\gamma = 1.4$. Hence, the value of K correspond to 3. In the equilibrium state, λ is related to the macroscopic variables $(\rho, \rho U, \rho V, \rho \varepsilon)$ through the relation,

$$\lambda = \frac{K+2}{4} \frac{\rho}{\rho \varepsilon - \frac{1}{2}\rho\left(U^2 + V^2\right)}, \tag{6}$$

The pressure p is related to ρ and λ through the following relation,

$$p = \frac{\rho}{2\lambda} \tag{7}$$

The relation between the gas distribution function f and the macroscopic variables is given by

$$W = (\rho, \rho U, \rho V, \rho\varepsilon)^T = \int \psi_\alpha f \, dudvd\xi , \tag{8}$$

where $d\xi = d\xi_1 d\xi_{2...} d\xi_K$, and

$$\psi_\alpha = \left(1, u, v, \tfrac{1}{2}\left(u^2 + v^2 + \xi^2\right)\right)^T , \tag{9}$$

are known as the moments.

The fluxes for the corresponding macroscopic variables could also be obtained using similar approach as above and is given as

$$F(W) = \left(F_\rho, F_{\rho U}, F_{\rho V}, F_{\rho\varepsilon}\right)^T = \int u\psi_\alpha f \, dudvd\xi \tag{10}$$

$$G(W) = \left(G_\rho, G_{\rho U}, G_{\rho V}, G_{\rho\varepsilon}\right)^T = \int v\psi_\alpha f \, dudvd\xi$$

In addition, the conservation principle for mass, momentum, and energy during the course of particle collisions requires $Q(f, f)$ to satisfy the compatibility condition

$$\int Q(f, f)\psi_\alpha \, dudvd\xi = 0, \qquad \alpha = 1,2,3. \tag{11}$$

The finite volume gas-kinetic scheme for the 2-D case is derived as

$$W_i^{n+1} = W_i^n - \frac{\Delta t}{\Delta x}\left(F_{i+1/2,j} - F_{i-1/2,j}\right) - \frac{\Delta t}{\Delta y}\left(G_{i,j+1/2} - G_{i,j-1/2}\right), \tag{12}$$

where Δt the step size in time, Δx and Δy the mesh size in x- and y-direction, while $F_{i+1/2,j}$ and $G_{i,j+1/2}$ are the numerical fluxes across cell interfaces.

3 NUMERICAL SCHEME

In this section, the first- and second-order two-dimensional BGK scheme would be considered. The scheme uses the fact that the Euler equations are the moments of the Boltzmann equation when the distribution function is Maxwellian. The first-order collisional scheme or better known, as the BGK scheme will be developed first. Lastly, a method of extending the first-order scheme to second-order will be reviewed.

3.1 1st-order BGK scheme

The BGK scheme is based on the Boltzmann equation with existing collision term, in which the collision term could be simplified to a form similar to that found in Eq. (3). Thus, the governing equation for the BGK scheme is expressed as [5]

$$f_t + uf_x + vf_y = \frac{g - f}{\tau} \tag{13}$$

Equation (13) with the collision term described by Eq. (3) is known as the BGK model of the Boltzmann equation. From Eq. (13), it can be shown that the compatibility condition (11) naturally becomes

$$\int \frac{g-f}{\tau}\psi_\alpha \, dudvd\xi = 0, \qquad \alpha = 1,2,3. \tag{14}$$

The general solution of f of the BGK model at the cell interface ($x_{i+1/2}$, y_j) is obtained as

$$f(x,y,t,u,v,\xi) = \frac{1}{\tau}\int_0^t g(x',y',t,u,v,\xi)e^{-(t-t')/\tau}dt' + e^{-t/\tau} f_o(x-ut, y-vt), \tag{15}$$

where $x' = x_{i+1/2} - u(t-t')$ and $y' = y_j - v(t-t')$ are particle trajectories and f_o is the initial non-equilibrium distribution function at $t = 0$.

For the initial condition of two constant states around a cell interface, $x_{i+1/2,j}$,

$$\begin{aligned} f_o &= \begin{cases} g_i, & u > 0 \\ g_{i+1}, & u < 0 \end{cases} \\ &= g_{i,j}H(u) + g_{i+1,j}(1+H(u)) \end{aligned} \tag{16}$$

where $H(u)$ is a Heaviside function. With the assumption of constant equilibrium state g_o in space and time, the solution f of the BGK model given by Eq. (15) can be expressed as follows:

$$\begin{aligned} f_{i+1/2,j} &= (1-e^{-t/\tau})g_O + e^{-t/\tau} f_O \\ &= (1-e^{-t/\tau})g_O + e^{-t/\tau}\left(g_{i,j}H(u) + g_{i+1,j}(1+H(u))\right) \end{aligned} \tag{17}$$

In the current 1st-order BGK scheme, the term $e^{-t/\tau}$ is assumed to be a constant and is denoted by the symbol η, where $\eta \in [0,1]$. Thus, the final distribution function at the cell interface $x_{i+1/2,j}$ for the BGK scheme could be interpreted as

$$f_{i+1/2,j} = (1-\eta)g_O + \eta f_O \tag{18}$$

The equilibrium state g_O could be defined by applying the compatibility condition (14) at the cell interface $x_{i+1/2,j}$ which yields,

$$\begin{aligned} &\int \psi_\alpha g_O \, dudvd\xi = \int \psi_\alpha f_O \, dudvd\xi \\ &\begin{pmatrix} \overline{\rho} \\ \overline{\rho U} \\ \overline{\rho V} \\ \overline{\rho \varepsilon} \end{pmatrix}_{i+1/2,j} = \int_{u>0} \psi_\alpha g_{i,j} \, dudvd\xi \quad + \quad \int_{u<0} \psi_\alpha g_{i+1,j} \, dudvd\xi \end{aligned} \tag{19}$$

Where the corresponding average macroscopic flow variables $(\overline{\rho}, \overline{\rho U}, \overline{\rho V}, \overline{\rho \varepsilon})$ at the cell interface could be determined by evaluating the moments of the equilibrium state in Eq. (19).

Therefore, the final numerical fluxes across the cell interface could be determined by using Eq. (10) and Eq. (18) which yields the following relations,

$$F_{i+1/2,j} = (1-\eta)F^e_{i+1/2,j} + \eta F^f_{i+1/2,j} \tag{20}$$

where $F^{e}_{i+1/2,j}$ is the equilibrium flux function and $F^{f}_{i+1/2,j}$ is the non-equilibrium or free stream flux function. For the numerical flux, $G_{i,j+1/2}$ across the cell interface between cells (i,j) and $(i,j+1)$, similar techniques can be used.

3.2 2nd-order BGK scheme

In order to extend the 1st-order BGK scheme to 2nd-order, a method known as the MUSCL-type approach is adopted [1,4]. The requirement for any high-order scheme required that interpolation technique be used in the reconstruction of the cell averaged mass, momentum, and energy densities. Thus, a linear approximation of the initial data on each cell is equivalent to a second-order space discretization. In addition, the *TVD* shock capturing properties of the high-resolution scheme are achieved via the use of non-linear limiter. In this extension, a minmod limiter is used to obtain a piecewise linear representation of the cell averaged macroscopic variables. Hence, the left and right states of the conservative variables at a cell interface $x_{i+1/2,j}$ could be obtained through the non-linear reconstruction of the initial data and are given as

$$\begin{aligned} W^{L}_{i+1/2,j} &= W_{i,j} + \frac{1}{2}\psi^{L}\left(W_{i,j} - W_{i-1,j}\right) \\ W^{R}_{i+1/2,j} &= W_{i+1,j} - \frac{1}{2}\psi^{R}\left(W_{i+1,j} - W_{i,j}\right) \end{aligned} \tag{21}$$

where the superscripts L, and R correspond to the left and right side at a considered cell interface. While, ψ^{L}, and ψ^{R} are the minmod limiters, which are given by

$$\begin{aligned} \psi^{L} &= \max\left(0, \min\left(1, r^{L}\right)\right) \\ \psi^{R} &= \max\left(0, \min\left(1, r^{R}\right)\right) \end{aligned} \tag{22}$$

where r^{L}, and r^{R} are given by

$$\begin{aligned} r^{L} &= \frac{W_{i+1,j} - W_{i,j}}{W_{i,j} - W_{i-1,j}} \\ r^{R} &= \frac{W_{i+1,j} - W_{i,j}}{W_{i+2,j} - W_{i+1,j}} \end{aligned} \tag{23}$$

From the reconstructed left and right states of the conservative variables, the second-order numerical fluxes across the cell interface could simply be evaluated using the formulation given by Eq. (20) for BGK scheme by understanding the following facts,

1st-order numerical flux: $F^{(1)}_{i+1/2,j} = F\left(W_{i,j}, W_{i+1,j}\right)$

2nd-order numerical flux: $F^{(2)}_{i+1/2,j} = F\left(W^{L}_{i+1/2,j}, W^{R}_{i+1/2,j}\right)$

In addition, a Runge-Kutta time stepping scheme is also adopted for the time integration method, where a three stage Runge-Kutta method of second-order accuracy in time is employed into the second-order gas-kinetic schemes and is given as [6],

$$W^{(1)} = W^n + \alpha_1 \Delta t L\left(W^n\right)$$
$$W^{(2)} = W^n + \alpha_2 \Delta t L\left(W^1\right), \tag{24}$$
$$W^{(n+1)} = W^n + \Delta t L\left(W^2\right)$$

with $\alpha_1 = 1/4, \alpha_2 = 1/2$. For the second-order scheme, the interpolated pressure jump p_l and p_r around a cell interface can naturally be used as a switch function for the parameter η, such as [4]

$$\eta = 1 - \exp\left(-\beta \frac{|p_l - p_r|}{p_l + p_r}\right), \tag{25}$$

where β can be some constant.

Similar procedures are followed in the reconstruction of initial data for 2nd-order numerical flux function $G_{i,j+1/2}$ across cell interfaces.

4 RESULTS AND DISCUSSIONS

4.1 Compressible inviscid regular shock reflection

This test case is a two dimensional compressible inviscid flow problem and it's taken from Ref. 3. The physical domain itself is rectangular of length 4 and height 1 divided into 60 x 20 rectangular grids with $\Delta x = 1/15$ and $\Delta y = 1/20$. Dirichlet conditions are imposed on the left and upper boundaries as

$$(\rho, U, V, p)\big|_{(0,y,t)} = (1.0, 2.9, 0.0, 1.0/4.0)$$
$$(\rho, U, V, p)\big|_{(x,1,t)} = (1.69997, 2.61934, -0.50633, 1.52819)$$

These conditions are based on the assumptions that the left boundary is a supersonic inflow condition while the upper boundary is set to satisfy the shock-jump relations with a shock angle equal to 29 degree. The bottom boundary is a reflecting wall and supersonic outflow condition is applied along the right boundary.

The integration in time is carried out until 1000 time steps, at which the solution reaches a steady state. The pressure contours as well as pressure distributions along the middle line in the y-direction for both 1st-order and 2nd-order schemes are shown in Fig. 1 to 6. The results for BGK scheme are compared with the results obtained from Roe's scheme. Figure 1 and 2 displayed the pressure contours for BGK and Roe's schemes at 1st-order accuracy, respectively, while Fig. 4 and 5 showed the pressure contours for both schemes at 2nd-order accuracy. Lastly, Fig. 3 and 6 showed the pressure distributions at centerline for both schemes with 1st- and 2nd-order accuracy, respectively. Examining the figures, one may say that there is a good agreement between the BGK and the Roe's schemes'. In addition to the numerical results for the pressure, the convergence histories of both schemes are also displayed in Fig. 7. From this figure, it clearly shows that the BGK scheme converges faster than the Roe's scheme. For a given 1000 time steps, the BGK scheme converges at 887 time iterations while the Roe's scheme converges at 906 time iterations.

5 CONCLUSION

From the Boltzmann equation, the gas-kinetic BGK scheme for the two-dimensional compressible inviscid flows is developed. The algorithms with 1st-order and 2nd-order accuracy are successfully applied to simulate two-dimensional flows. Analyzing the results revealed that the BGK scheme is able to produce numerical results that are comparable, robust, and as accurate as the Roe's scheme. In addition, the BGK scheme proved that it is more efficient than the Roe's scheme.

REFERENCES

[1] Hirsch, K., "The Numerical Computation of Internal and External Flows", John Wiley & Sons, Vol. 2 1990.

[2] Xu, K., "Entropy Analysis of Kinetic Flux Vector Splitting Schemes for the Compressible Euler Equations", ICASE Report, **99-5**, 1999.

[3] Xu, K., "Gas-Kinetic Scheme for Unsteady Compressible Flow Simulations", von Karman Institute for Fluid Dynamics Lecture Series, 1998-03, 1998.

[4] Xu, K., "Gas-Kinetic Theory Based Flux Splitting Method for Ideal Magnetohydrodynamics", ICASE Report, **98-53**, 1998.

[5] Xu, K., "A Gas-Kinetic BGK Scheme for the Compressible Navier-Stokes Equations", ICASE Report, **2000-38**, 2000.

[6] Choi, H. and Liu, J. G., "The Reconstruction of Upwind Fluxes for Conservation Laws: It's Behavior in Dynamic and Steady State Calculations", J. Comput. Phys., **144**, 237-256, 1998.

[8] Roe, P. L., "Approximate Riemann Solvers, Parameter Vectors and Difference Schemes", J. Comput. Phys., **43**, 357-372, 1981.

[9] Ruan, Y. and Jameson, A., "Gas-Kinetic BGK Method for Three-Dimensional Compressible Flows", AIAA Paper, 2002-0550, 2002.

[10] Chae, D. S., Kim, C. A and Rho, O. H., "Development of an Improved Gas-Kinetic BGK Scheme for Inviscid and Viscous Flows", J. Comput. Phys., Vol. 158, PP 1-27, 2000.

[11] Ong, J. C., Omar, A. A. and Waqar, A., "The Accuracy of Gas-Kinetic Schemes for Solving Compressible Inviscid Flow Problems", International Conference on Scientific and Engineering Computation, Singapore, Dec. 2002.

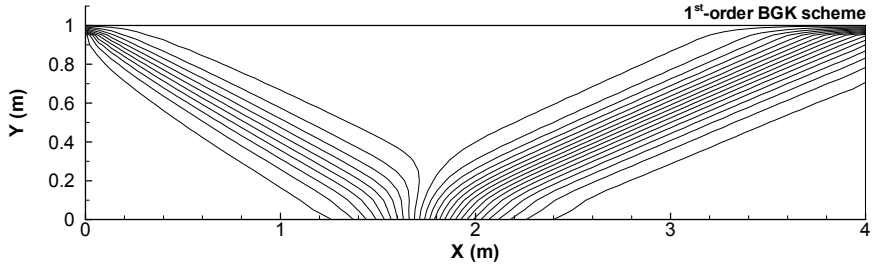

Figure 1: Pressure contours for the 1st-order BGK scheme.

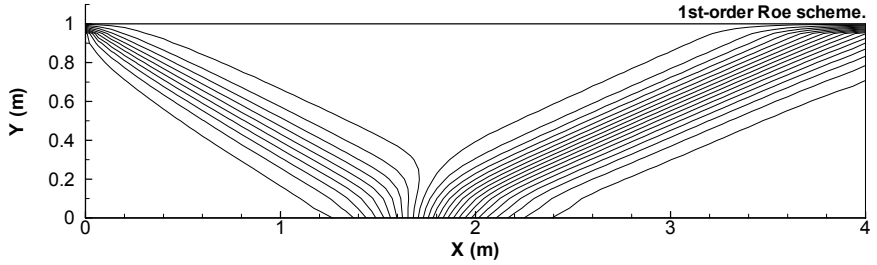

Figure 2: Pressure contours for the 1st-order Roe's scheme.

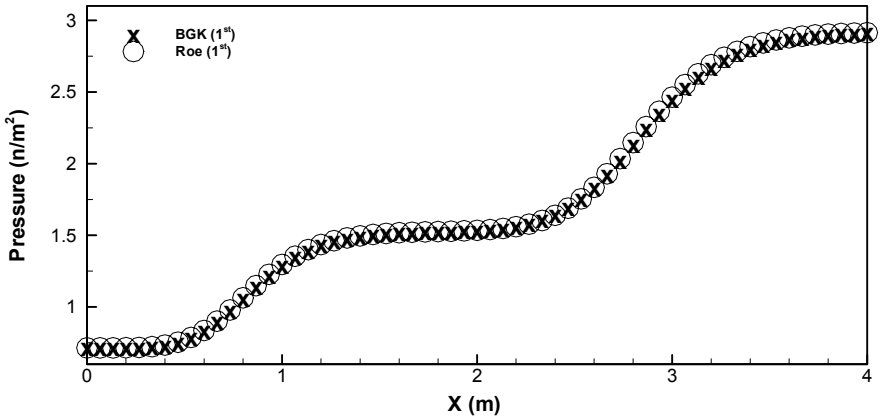

Figure 3: Pressure distribution at the centerline for 1st-order BGK and Roe's schemes.

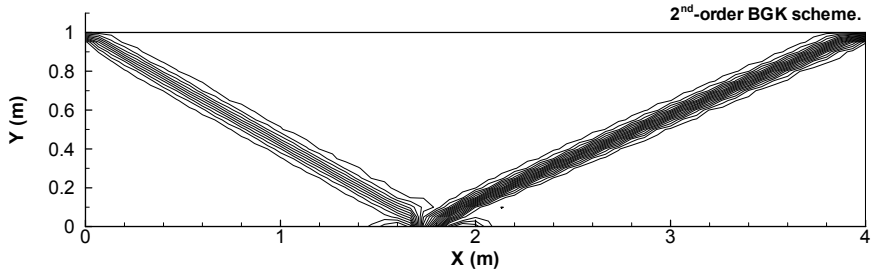

Figure 4: Pressure contours for the 2nd-order BGK scheme.

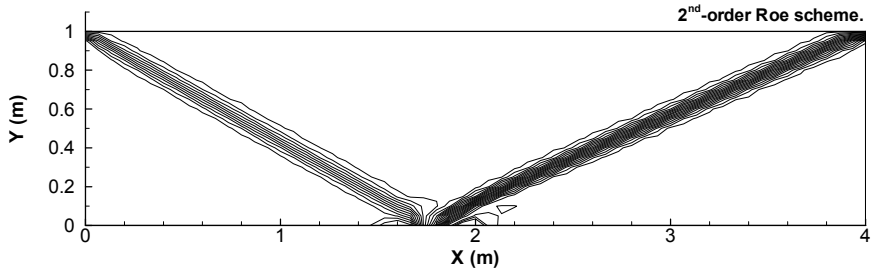

Figure 5: Pressure contours for the 2nd-order Roe's scheme.

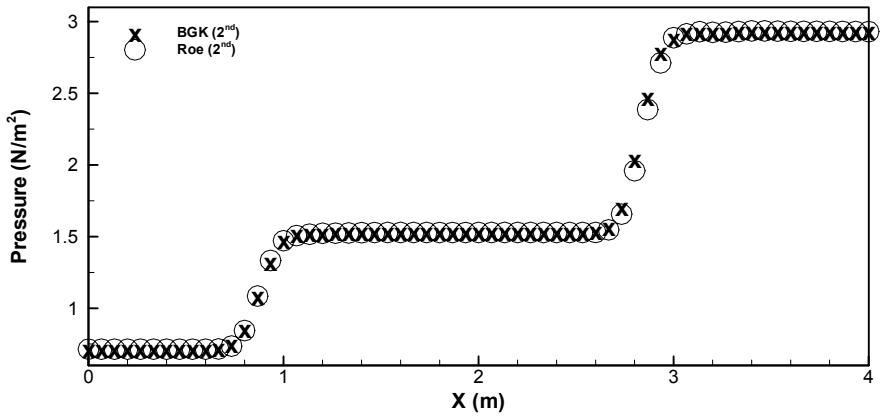

Figure 6: Pressure distribution at the centerline for 2nd-order BGK and Roe's schemes.

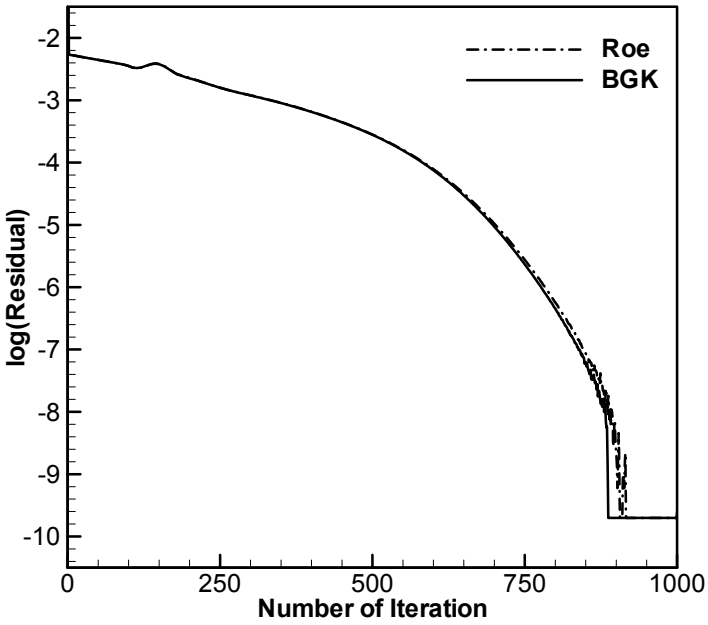

Figure 7: Convergence history of the residual of pressure with the Roe's and BGK schemes.